

Studies on properties of the xylan-binding domain and linker sequence of xylanase XynG1-1 from *Paenibacillus campinasensis* G1-1

Yihan Liu^{1,2,3,4} · Lin Huang^{1,2,3,4} · Weiguo Li^{1,2,3,4} · Wei Guo^{1,2,3,4} · Hongchen Zheng^{1,2,3,4} · Jianling Wang^{1,2,3,4} · Fuping Lu^{1,2,3,4}

Received: 20 July 2015 / Accepted: 28 September 2015 / Published online: 14 October 2015
© Society for Industrial Microbiology and Biotechnology 2015

Abstract Xylanase XynG1-1 from *Paenibacillus campinasensis* G1-1 consists of a catalytic domain (CD), a family 6₃₆ carbohydrate-binding module which is a xylan-binding domain (XBD), and a linker sequence (LS) between them. The structure of XynG1-3 from *Bacillus pumilus* G1-3 consists only of a CD. To investigate the functions and properties of the XBD and LS of XynG1-1, two truncated forms (XynG1-1CDL, XynG1-1CD) and three fusion derivatives (XynG1-3CDL, XynG1-3CDX and XynG1-3CDLX) were constructed and biochemically characterized. The optimum conditions for the catalytic activity of mutants of XynG1-1 and XynG1-3 were 60 °C and pH 7.0, and 55 °C and pH 8.0, respectively, the same as for the corresponding wild-type enzymes. XynGs with an XBD were stable over a broad temperature (30–80 °C) and pH range (4.0–11.0), respectively, on incubation for 3 h. Kinetic parameters (K_m , k_{cat} , k_{cat}/K_m) of XynGs were determined with soluble birchwood xylan and insoluble oat spelt xylan as substrates. XynGs with the XBD showed better affinities toward, and more efficient catalysis of hydrolysis of the insoluble substrate. The XBD had

positive effects on thermostability and pH stability and a crucial function in the ability of the enzyme to bind and hydrolyze insoluble substrate. The LS had little effect on the overall stability of the xylanase and no relationship with affinities for soluble and insoluble substrates or catalytic efficiency.

Keywords Xylanase · Carbohydrate-binding module · Xylan-binding domain · Linker sequence · Enzyme properties

Background

Xylanases (endo-1,4- β -d-xylanohydrolases; E.C. 3.2.1.8) are key microbial enzymes for the degradation of the backbone of xylan by hydrolyzing β -1,4-xylosidic linkages between two d-xylopyranosyl residues [12, 17, 24]. Xylanases have been found that contain a catalytic domain (CD) and ancillary modules such as non-catalytic carbohydrate-binding modules (CBMs), which are present in many types of glycoside hydrolase and are classified into different families based on amino acid sequence similarities (<http://www.cazy.org>). Parts of CBMs bind specifically to long xylan chains and as such are defined as xylan-binding domains (XBDs) [19].

Several xylanases are reported to have XBDs that affect the thermostability of the enzymes and binding abilities with insoluble substrates. For example, the absence of the XBD resulted in a decrease in the thermostability of XynA from *Caldibacillus cellulovorans* [20]. The XBD in XynX from *Clostridium thermocellum* has been suggested to have dual functions, thermostabilization and binding of xylan [18]. The XBD and linker sequence (LS) (located between the CD and XBD) from *Thermomonospora fusca* xylanase

Y. Liu and L. Huang contributed equally to this study.

✉ Fuping Lu
lfp@tust.edu.cn

- ¹ Key Laboratory of Industrial Fermentation Microbiology, Ministry of Education, Tianjin 300457, China
- ² Tianjin Key Laboratory of Industrial Microbiology, Tianjin 300457, China
- ³ National Engineering Laboratory for Industrial Enzymes, Tianjin 300457, China
- ⁴ The College of Biotechnology, Tianjin University of Science and Technology, Tianjin 300457, China

A have important roles in the binding and hydrolysis of insoluble substrates [13]. In our previous work, we showed that XynG1-1 from *Paenibacillus campinasensis* G1-1, isolated from a Chinese paper mill, consisted of a CD and CBM6_36 [25]. This binding module, CBM6_36, contained CBM36 and CBM6 in its general structure and was primarily a xylan-binding CBM (i.e., an XBD) [8]. The CD and XBD of XynG1-1 were linked together through LS. XynG1-1 exhibited high stability at temperatures 70–80 °C and across a wide range of pHs (pH 5.0–9.0), and a significant binding ability with insoluble substrates. These properties made XynG1-1 suitable for industrial purposes such as bioethanol production and pulp bioleaching [26]. Meanwhile, another xylanase, XynG1-3, containing only a single CD, was obtained from *Bacillus pumilus* G1-3 (TCCC11579). The construction of forms of xylanase in which (1) XynG1-1 is truncated to resemble XynG1-3, and (2) an XBD and LS were fused to XynG1-3 to produce a product that resembles XynG1-1 may provide new insight into the structure–function relationship of xylanase.

In this study, XynG1-1 was truncated in the XBD and LS, respectively. Then, the XBD, LS and XBD+LS were, respectively, fused to the C-terminus of XynG1-3. Two wild-type (WT) xylanases, XynG1-1 and XynG1-3, and five corresponding derivatives were investigated and compared in depth to reveal the roles of the XBD and LS in the thermostability, pH stability and catalytic activities of xylanases.

Materials and methods

Plasmids, bacterial strains and growth conditions

Plasmid pET-22b(+) was preserved in our laboratory and plasmids pET-XynG1-1 and pET-XynG1-3, respectively, harboring XynG1-1 and XynG1-3 were obtained from our previous work [25, 26]. *Escherichia coli* DH5 α and *E. coli* BL21 (DE3) were conserved in our laboratory for vector propagation and expression, respectively. Recombinant strains were grown at 37 °C in Luria–Bertani (LB) broth supplemented with ampicillin (Amp) at 100 $\mu\text{g mL}^{-1}$.

Construction of the recombinants

The plasmids pET-XynG1-1 and pET-XynG1-3 were used as the main templates for PCR amplifications of DNA sequences encoding mutant XynGs. The PCR primers are shown in Table 1. XynG1-ICDL and XynG1-ICD were amplified from plasmid pET-XynG1-1 containing the full-length XynG1-1 by general PCR with conditions as follows: 95 °C for 5 min, followed by 30 cycles of 45 s at 94 °C, 45 s at 55 °C and 90 s at 72 °C, with a

final extension for 10 min at 72 °C. The genes XynG1-3CDX and XynG1-3CDLX were amplified by overlapping PCR. Overlapping PCR was carried out with two rounds of amplification. In the first round, full-length XynG1-3 and the gene fragments encoding the XBD and XBD+LS were amplified using corresponding primer sets P1–P2 and P3–P4, respectively. In the second round, corresponding primers P1 and P4 were used to amplify XynG1-3CDX and XynG1-3CDLX using the products of the primary reactions as the templates. The overlapping PCR conditions were the same as for general PCR. General PCR and the second round of overlapping PCR were carried out using Taq DNA polymerase (Tiangen, Hai Dian District, Beijing, China) and high fidelity Pyrobest DNA polymerase (Takara, Japan) was used in the first round of overlapping PCR. DNA fragments were digested by HindIII (Takara) and XhoI (Takara), and ligated into pET22b(+) previously digested with the same restriction enzymes. The plasmids constructed were named pET-XynG1-1CDL, pET-XynG1-1CD, pET-XynG1-3CDX, and pET-XynG1-3CDLX, respectively. Finally, XynG1-3CDL was obtained by general PCR using pET-XynG1-3CDLX as the template and plasmid pET-XynG1-3CDL was generated following the construction steps described above. Subsequently, the recombinant plasmids were transformed into *E. coli* DH5 α for propagation. Then, the isolated plasmids were checked by sequencing of the inserted DNA fragments.

Expression and purification of the recombinant XynGs

Plasmids were transformed into the expression host *E. coli* BL21. Transformants harboring the recombinant plasmids were cultivated overnight in LB broth supplemented with Amp (100 $\mu\text{g mL}^{-1}$) at 37 °C. Then, 2 % (v/v) overnight culture was transferred into 50 mL of LB broth (containing Amp 100 $\mu\text{g mL}^{-1}$) in a 250 mL flask with constant shaking at 180 rpm for 2–3 h. Protein production was induced by the addition of IPTG to a final concentration of 1 mM when the culture reached an optical density of 0.8–1.0 at 600 nm, then cultures were further cultivated with shaking at 100 rpm for 16–20 h (20 °C) to express WT and mutant XynGs. The extracellular proteins were collected by centrifugation at 4000 \times g for 10 min and liquid supernatants were applied to Ni⁺ NTA agarose (Novagen, Madison, WI, USA) columns equilibrated with buffer (300 mM NaCl, 50 mM sodium phosphate, pH 7.0). Subsequently, WT and mutant XynGs were eluted with a linear imidazole gradient of 20–150 mM in the same buffer. Enzyme purification was evaluated by SDS-PAGE. Protein concentrations were estimated by the Bradford assay (Bio-Rad) using bovine serum albumin as a standard [2].

Table 1 Gene names, descriptions, templates, primers for molecular modification

Gene names	Descriptions	Templates	Primers and sequences	PCR type
<i>XynGI-1</i>	WT <i>XynGI-1</i>	pET- <i>XynGI-1</i>	<u>XynGI-1 P1</u> 5'-CCCAAGCTTGCACCACGATCACTTCTAACGAGA-3' <u>XynGI-1 P2</u> 5'-CCGCTCGAGCCGGATCTCCAAATAGTCAATG-3'	General PCR
<i>XynGI-1CDL</i>	<i>XynGI-1</i> without <i>XBD</i>	pET- <i>XynGI-1</i>	<u>XynGI-1CDL P1</u> 5'-CCCAAGCTTGCACCACGATCACTTCTAACGAGA-3' <u>XynGI-1CDL P2</u> 5'-CCGCTCGAGCGTTCCCGGGTTCGTGCCTC-3'	General PCR
<i>XynGI-1CD</i>	<i>XynGI-1</i> without <i>XBD</i> and <i>LS</i>	pET- <i>XynGI-1</i>	<u>XynGI-1CD P1</u> 5'-CCCAAGCTTGCACCACGATCACTTCTAACGAGA-3' <u>XynGI-1CD P2</u> 5'-CCGCTCGAGGCTGTACACATTCGCGCTTC-3'	General PCR
<i>XynGI-3</i>	WT <i>XynGI-3</i>	pET- <i>XynGI-3</i>	<u>XynGI-3 P1</u> 5'-CCCAAGCTTAGAACCAATTACGAATAATGAAATG-3' <u>XynGI-3 P2</u> 5'-CCGCTCGAGGTTGCCAATAAACAGCTGATTG-3'	General PCR
<i>XynGI-3CDX</i>	<i>XynGI-3</i> with <i>XBD</i> of <i>XynGI-1</i>	pET- <i>XynGI-3</i> and pET- <i>XynGI-1</i>	<u>XynGI-3CDX P1</u> 5'-CCCAAGCTTAGAACCAATTACGAATAATGAAATG-3' <u>XynGI-3CDX P2</u> 5'-ITCAGCTTCGACTCTCGTCACGTTGCCAATAACA-3' <u>XynGI-3CDX P3</u> 5'-CTGTTTATTGGCAACGTGACGAGAGTCGAAAGCTG-3' <u>XynGI-3CDX P4</u> 5'-CCGCTCGAGCCGGATCTCCAAATAGTCAATG-3'	Overlapping PCR
<i>XynGI-3CDLX</i>	<i>XynGI-3</i> with <i>XBD</i> and <i>LS</i> of <i>XynGI-1</i>	pET- <i>XynGI-3</i> and pET- <i>XynGI-1</i>	<u>XynGI-3CDLX P1</u> 5'-CCCAAGCTTAGAACCAATTACGAATAATGAAATG-3' <u>XynGI-3CDLX P2</u> 5'-CCCGCCGATGGTCAATGTATTGTTGCCAATAACA-3' <u>XynGI-3CDLX P3</u> 5'-CTGTTTATTGGCAACAATACATTGACCATCGGGGG-3' <u>XynGI-3CDLX P4</u> 5'-CCGCTCGAGCCGGATCTCCAAATAGTCAATG-3'	Overlapping PCR
<i>XynGI-3CDL</i>	<i>XynGI-3</i> with <i>LS</i> of <i>XynGI-1</i>	pET- <i>XynGI-3CDLX</i>	<u>XynGI-3CDL P1</u> 5'-CCCAAGCTTAGAACCAATTACGAATAATGAAATG-3' <u>XynGI-3CDL P2</u> 5'-CCGCTCGAGCGTTCCCGGGTTCGTGCCTC-3'	General PCR

Underlined indicates *Hind*III and *Xho*I sites, respectively

Xylanase assay

The activities of recombinant XynGs were determined by the amount of reducing sugar produced using the 3,5-dinitrosalicylic acid method, with birchwood xylan (Sigma) or oat spelt xylan (Sigma) as substrates [1]. The reaction system consisted of 100 μ L of 1 % (w/v) birchwood xylan in sodium phosphate buffer (20 mM, pH 7.0), with which 100 μ L of appropriately diluted enzyme extract was incubated at 60 °C for 10 min. The reaction was ended by the addition of 600 μ L 3,5-dinitrosalicylic acid and then the mixture was placed in a boiling water bath for 10 min. Control samples contained the same reagents except enzyme and the same reaction steps were performed. Thereafter, reaction liquid was cooled to room temperature and measured against the control at 540 nm in a spectrophotometer. One unit of xylanase activity was defined as the amount of enzyme that released 1 μ mol of reducing sugar from the birchwood xylan or oat spelt xylan per minute under the assay conditions. Each assay was performed in triplicate.

Characterization of recombinant XynGs

The optimum temperatures and pHs for activity of WT and mutant XynGs were measured by assaying the xylanase activities at different temperatures (40–80 °C) and pHs (4.0–11.0). Sodium acetate buffer (pH 4.0–5.0), sodium phosphate (pH 6.0–7.0), Tris–HCl (pH 8.0–9.0) and glycine–NaOH (pH 10.0–11.0) were used as buffers at the concentrations of 20 mM. The relative enzymatic activity was calculated as a percentage of the maximal activity.

For measuring thermal stabilities, the residual activities of XynG1-1s and XynG1-3s were determined at the optimal pH after incubation for 3 h at temperatures ranging from 30 to 80 °C. Similarly, to assess pH stabilities, XynG1-1s and XynG1-3s were pre-incubated at various pHs (pH 4.0–11.0) for 3 h in the absence of substrate, and then the residual activities were measured at the respective optimal temperatures. Residual activities were calculated as percentages of the initial activities. The kinetic parameters K_m , k_{cat} and k_{cat}/K_m of purified WT and mutant XynGs were estimated from Lineweaver–Burk double reciprocal plots of xylanase activities. The activities of XynGs were measured using different concentrations (0.1–1.0 % w/v) of birch xylan and oat spelt xylan (Sigma) as soluble and insoluble substrates, respectively, in optimal reaction conditions, for 10 min.

Computer modeling methods

To obtain the theoretical structures of WT and mutant XynGs, models of XynGs were generated using the

Swiss-Model server, with *Bacillus* sp. 41M-1 xylanase J (PDB code: 2dcj) as the template. Three-dimensional structures of WT and mutant XynGs were drawn using the PyMOL molecular graphics system.

Results and discussion

Gene cloning and construction of expression vectors

Nucleotide sequence analysis confirmed that XynG1-1 consisted of 196 amino acids in the CD, 23 amino acids in the LS and 119 amino acids in the XBD. XynG1-3 only contained a 201-amino acid CD. Mutant xylanases genes, i.e., *XynG1-1CDL* (657 bp), *XynG1-1CD* (588 bp), *XynG1-3CDL* (672 bp), *XynG1-3CDX* (960 bp) and *XynG1-3CDLX* (1029 bp), were constructed by general and overlapping PCR. Figure 1 shows details of the modified gene products and their nomenclature. The sequences of mutant genes *XynG1-3CDX*, *XynG1-3CDLX* and *XynG1-3CDL* were uploaded to the NCBI databases and their accession numbers in GenBank are JQ965923.1, JQ965922.1 and JQ965924.1, respectively. The DNA fragments were cloned into vector pET22b(+) to obtain plasmids pET-*XynG1-1CDL*, pET-*XynG1-1CD*, pET-*XynG1-3CDX*, pET-*XynG1-3CDLX* and pET-*XynG1-3CDL*.

Expression, purification and 3-D structure of XynGs

After confirming the mutant plasmids by DNA sequencing, the vectors were transformed into *Escherichia coli* BL21 for protein expression. WT and mutant XynGs were purified by Ni²⁺-NTA affinity chromatography and purified proteins and their molecular masses were assayed by SDS-PAGE. The molecular masses of XynG1-1, XynG1-1CDL, XynG1-1CD, XynG1-3, XynG1-3CDL, XynG1-3CDX and XynG1-3CDLX banded on 12 % SDS-PAGE were 41, 25, 24, 24, 25, 40 and 41 kDa, respectively (data not shown), which were close to the theoretical values. Purified XynGs formed a single band with purity at least 95 %, respectively, and were thus suitable for functional analysis.

To explore the differences between WT and mutant XynGs, three-dimensional structure models of WT and mutant XynGs were built using the Swiss-Model (<http://www.expasy.ch/swissmod/SWISS-MODEL.html>) and PyMOL molecular graphics systems with *Bacillus* sp. 41M-1 xylanase J (PDB code: 2dcj) as the template (Fig. 2).

Characterization of XynGs

In the previous study, the characterizations of purified XynG1-1 and XynG1-3 with his-tagged showed that it

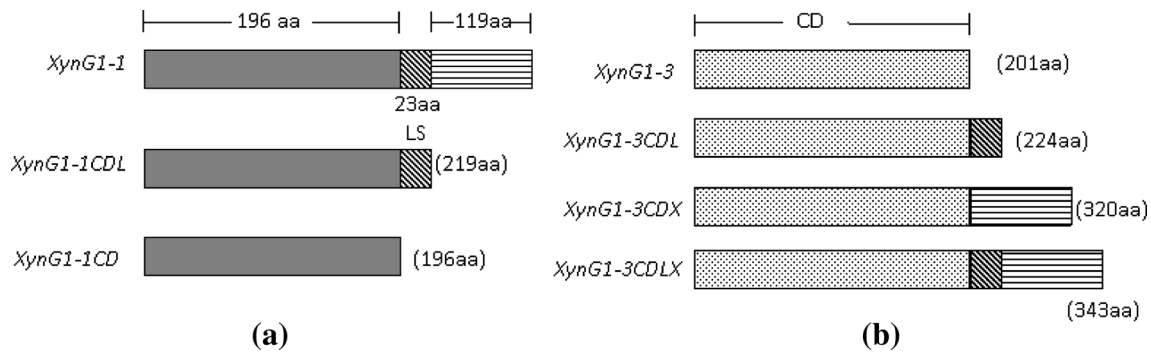


Fig. 1 Diagrammatic representation of the domains encoded by gene products in this work. **a** Domain architecture and length of XynG1-1 truncated derivatives. XynG1-1CDL was truncated in the XBD of XynG1-1. XynG1-1CD was truncated in the XBD and LS of XynG1-1. **b** Domain architecture and length of XynG1-3 con-

structed derivatives. XynG1-3 CDL was XynG1-3 fused with the LS of XynG1-1. XynG1-3CDX was XynG1-3 joined with the XBD of XynG1-1. XynG1-3CDLX was XynG1-3 fused with the XBD and LS of XynG1-1

was similar to the purified XynG1-1 and XynG1-3 from *P. campinasensis* G1-1 and *B. pumilus* G1-3 using the traditional purification method [culture filtrate, $(\text{NH}_4)_2\text{SO}_4$ precipitation, octyl-Sepharose, Sephadex G75] (data not shown), respectively. These findings indicated that his-tagged in our research would not affect either the catalytic activities or stabilities of the enzymes.

As Fig. 3a, b shows, XynG1-1 and its variants displayed their highest activities at 60 °C and pH 7.0. Loss of the XBD and LS had small, negative effects on enzyme activities at higher or lower temperatures than this optimum. Meanwhile, the activities of mutant XynG1-1s were lower than that of the WT at alkaline pHs (Fig. 3b). Thermostability assays showed that the residual activities of WT XynG1-1 after 3 h of incubation at 60 and 80 °C were 58 and 33 %, respectively (Fig. 3c). XynG1-1CDL and XynG1-1CD lost their activities completely after 3 h of incubation at 60 °C. Furthermore, the residual activity of XynG1-1CD decreased more than that of XynG1-1CDL at 40 and 50 °C. On analysis of the effects of pH, mutant XynG1-1s displayed not only their highest activities but also high stabilities at pH 7.0, where they retained at least 90 % of their maximal activity after 3 h incubation; the mutant XynG1-1s were less stable than the WT with respect to treatment at acidic or alkaline pHs (Fig. 3d).

Optimum conditions for activity of XynG1-3s were 55 °C (Fig. 4a) and pH 8.0 (Fig. 4b). Assaying for thermostability, XynG1-3 and XynG1-3CDL retained no activity after incubation at 60 °C for 3 h, while XynG1-3CDX and XynG1-3CDLX retained around 10 and 16 % residual activities, respectively (Fig. 4c). Thus, the XBD of XynG1-1 had some positive effect on the thermostability of XynG1-3, in accord with the results described above and in Fig. 3 on truncation of XynG1-1. In pH stability analysis,

mutant XynGs fused with the XBD showed enhanced stabilities under alkaline and acidic conditions and showed a wide pH tolerance between pH 4.0 and 11.0, whereas the LS had almost no effect on pH stability (Fig. 4d).

As stated above, the optimum temperature and pH properties of mutant XynGs in catalysis were not changed compared with the WT XynGs. The absence or presence of an XBD had a significant effect on the thermal stabilities of the mutant enzymes compared with the respective WT enzymes. The XBD was, therefore, suggested to have an important positive effect on thermostability, similar to observations in several previous reports [9, 15, 18]. Meanwhile, the LS also played a role in thermostability. In addition, we found a novel function of the XBD in pH stability, which could be useful for industrial applications [11, 21, 27].

Kinetic parameters of XynGs

The K_m , k_{cat} and k_{cat}/K_m values of purified WT and mutant XynGs using birchwood xylan and oat spelt xylan as soluble and insoluble substrates, respectively, were displayed in Table 2. The K_m values for XynG1-1, XynG1-1CDL and XynG1-1CD were 5.86, 6.58 and 6.49 mg mL^{-1} for birchwood xylan, which revealed that XynG1-1 had a higher binding affinity than XynG1-1CDL and XynG1-1CD for soluble substrate. Mutant XynG1-3s fused with the XBD had higher affinities toward soluble birchwood than XynG1-3 and XynG1-3CDL. The k_{cat}/K_m values of mutants of XynG1-1s were decreased by deletion of the XBD, and for mutant XynG1-3s with an XBD, the k_{cat}/K_m values were increased 1.5-fold relative to WT XynG1-3, indicating that XynGs with an XBD had a higher catalytic ability to hydrolyze birchwood. Similar results have been reported in the literature [13,

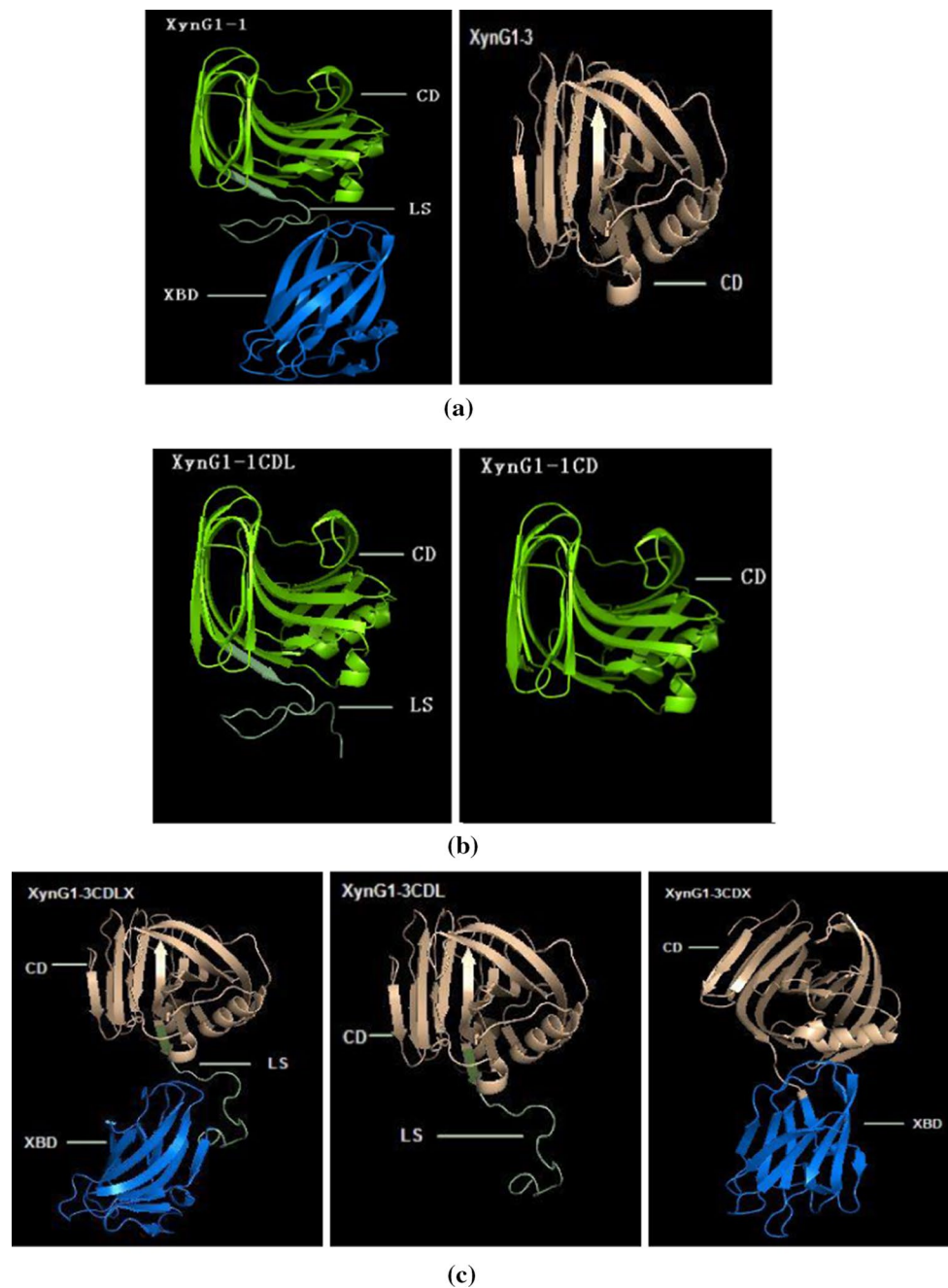


Fig. 2 Three-dimensional structure models of the WT and mutant XynGs. **a** Structures of WT XynGs. **b** Structures of mutants of XynG1-1. **c** Structures of mutants of XynG1-3. The CD of XynG1-1 is shown in *light green*. The LS of XynG1-1 is shown in *dark green*. The XBD of XynG1-1 is shown in *blue*. The CD of XynG1-3 is

shown in *brown*. Models of XynGs were generated using the Swiss-Model server, with *Bacillus* sp. 41M-1 xylanase J (PDB code: 2dcj) as the template. The structures of WT and mutant XynGs were rendered using the PyMOL molecular graphics system (color figure online)

15, 20, 23]. Previous research showed that the XBD and LS were important domains for hydrolyzing hemicelluloses from plant cell walls [4] and other complexes containing cellulose/hemicellulose [7]. The XBD could make enzymes bind well to plant cell wall material, and the LSs might facilitate the access of the CD to soluble xylan by providing flexibility [13].

The binding affinities of XynG1-1, XynG1-1CDL and XynG1-1CD toward insoluble substrate (oat spelt xylan) decreased in the order $K_m = 7.21 < 11.21 \approx 11.29 \text{ mg mL}^{-1}$, respectively, and for XynG1-3, XynG1-3CDL, XynG1-3CDX and XynG1-3CDLX increased in the order $K_m = 7.03 > 7.48 > 5.52 \approx 5.59 \text{ mg mL}^{-1}$ (Table 2). The catalytic

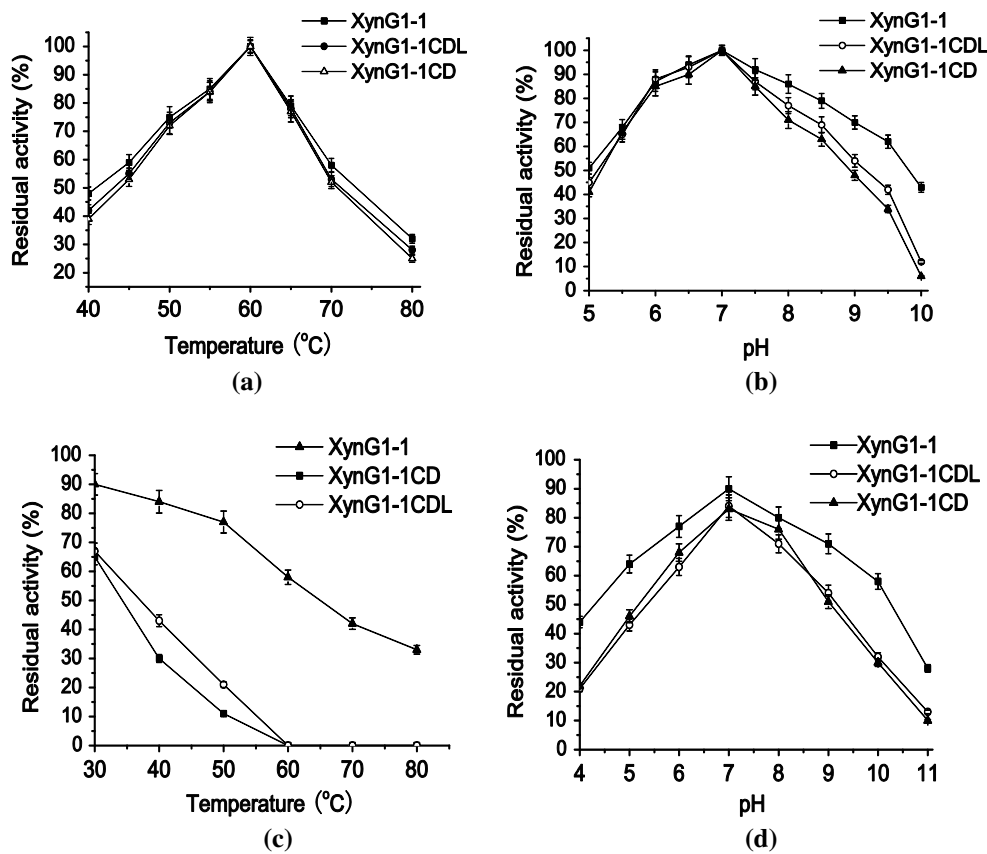


Fig. 3 Characterizations of WT and mutant XynG1-1s. **a** Determination of the optimum temperature for activity of WT and mutant XynG1-1s; **b** Determination of the optimum pH for activity of WT and mutant XynG1-1s; **c** Thermal stability of WT and mutant

XynG1-1s at various temperatures and pH 7.0; **d** pH stability of WT and mutant XynG1-1s at various pHs and 60 °C. Data are presented as mean ± SD (*n* = 3)

efficiencies (k_{cat}/K_m) of mutant XynG1-1s were decreased nearly two-fold compared with WT XynG1-1, while mutant XynG1-3s with the XBD had higher catalytic efficiencies than XynG1-3s without an XBD. Thus, the XBD was a crucial domain for the efficient hydrolysis of insoluble substrate, similar to previous observations [6, 10]. In the literature, members of the glycoside hydrolase family contained various CBMs, which had potential abilities to bind polysaccharides with different affinities [15, 20]. The k_{cat}/K_m value of XynG1-1 was higher than that of mutant XynG1-3s with the XBD added that might be due to the intrinsic properties of the catalytic domain, the structural arrangement between the substrate binding module and the CD, or both. XynG1-1 and XynG1-3s with an XBD had greater hydrolyzing abilities toward insoluble substrate than mutant XynG1-1s without the XBD or XynG1-3s without XBD, suggesting that XynGs need an XBD for efficient catalysis of insoluble xylan [5].

The LS had no significant effect on binding affinities or catalytic activities toward soluble and insoluble substrates in this study, which was similar to the report of

Brutus et al. [3]. However, some positive and negative effects have been found in the catalyzing ability of xylanases in previously published studies [14, 16, 22, 23]. On the basis of these observations, it appears that the different functions of LS towards substrates may result from the structures of the CD, LS, and CBM in various xylanases.

Conclusions

The XBD and the LS were studied by deletion from *P. campinasensis* GH11 XynG1-1 and addition into *B. pumilus* GH11 XynG1-3. The characterization and kinetic parameters of XynGs were compared, respectively. The results showed that the XBD of XynG1-1 had functions in thermostabilization, pH stability, binding and hydrolyzing ability towards insoluble substrate. Meanwhile, LS had little effect on the overall stability of the xylanase and no relationship with affinities for soluble and insoluble substrates or catalytic efficiency.

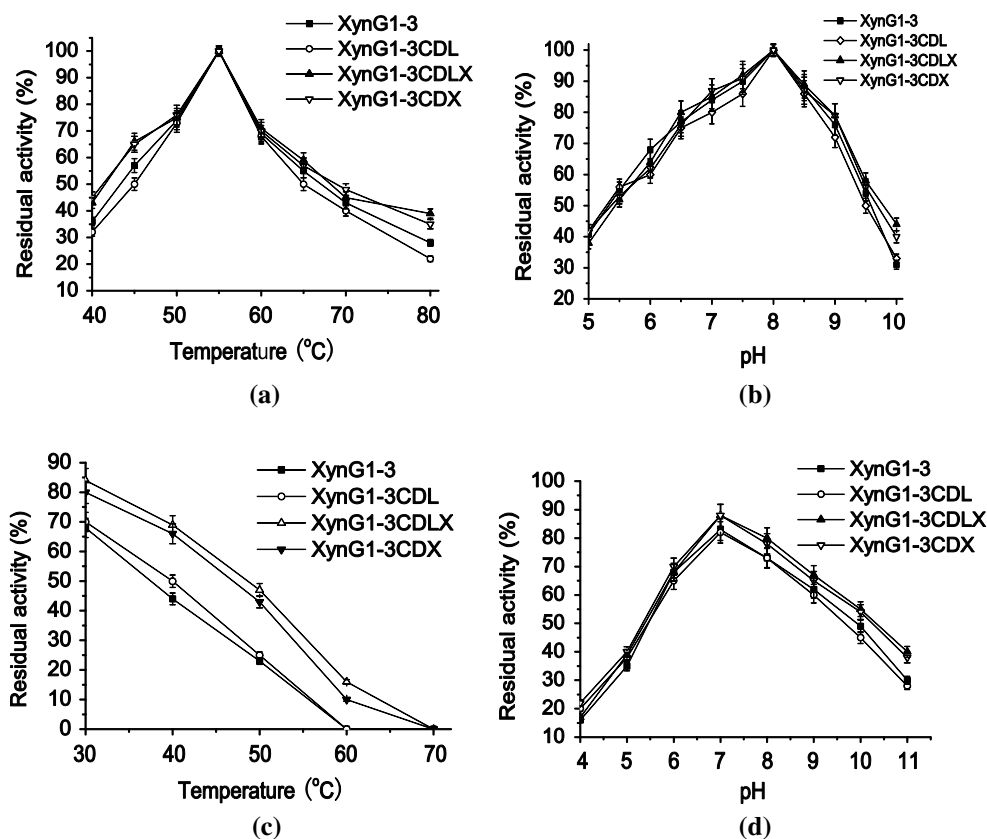


Fig. 4 Characterizations of WT and mutant XynG1-3s. **a** Determination of the optimum temperature for activity of WT and mutant XynG1-3s; **b** Determination of the optimum pH for activity of WT and mutant XynG1-3s; **c** Thermal stability of WT and mutant

XynG1-3s at various temperatures and pH 8.0; **d** pH stability of WT and mutant XynG1-3s at various pHs and 55 °C. Data are presented as mean \pm SD ($n = 3$)

Table 2 Kinetic parameters of XynGs toward birchwood xylan and oat spelt xylan

Protein name	Birchwood xylan			Oat spelt xylan		
	K_m (mg ml ⁻¹)	K_{cat} (s ⁻¹)	K_{cat}/K_m (ml mg ⁻¹ s ⁻¹)	K_m (mg ml ⁻¹)	K_{cat} (s ⁻¹)	K_{cat}/K_m (ml mg ⁻¹ s ⁻¹)
XynG1-1	5.86 \pm 0.23	1323.12 \pm 59.54	255.79 \pm 10.23	7.21 \pm 0.31	826.12 \pm 33.17	114.58 \pm 4.70
XynG1-1CDL	6.58 \pm 0.33	1102.32 \pm 49.60	167.53 \pm 7.54	11.21 \pm 0.43	634.26 \pm 24.77	56.58 \pm 2.37
XynG1-1CD	6.49 \pm 0.31	1093.24 \pm 49.23	168.45 \pm 7.41	11.29 \pm 0.51	623.94 \pm 29.41	55.26 \pm 2.14
XynG1-3	6.22 \pm 0.29	537.45 \pm 24.72	86.37 \pm 3.76	7.03 \pm 0.32	198.53 \pm 8.34	28.24 \pm 1.33
XynG1-3CDL	6.24 \pm 0.27	539.14 \pm 25.12	86.40 \pm 3.81	7.48 \pm 0.28	205.09 \pm 9.26	27.40 \pm 1.19
XynG1-3CDX	5.82 \pm 0.28	817.07 \pm 31.86	140.39 \pm 6.32	5.52 \pm 0.26	354.21 \pm 18.16	64.17 \pm 3.08
XynG1-3CDLX	5.88 \pm 0.30	825.85 \pm 32.52	140.45 \pm 6.45	5.59 \pm 0.28	367.98 \pm 18.77	65.83 \pm 3.17

Acknowledgments This work was supported by the National High-Tech Research and Development Plan (“863” Plan) (2012AA022108), the Tianjin Research Program of Application Foundation and Advanced Technology (14JCYBJC23800), and the Tianjin Support Plan Program of Science and Technology (14ZCZDSY00014).

References

- Bailey MJ, Biely P, Poutanen K (1992) Laboratory testing of method for assay of xylanase activity. *J Biotechnol* 23:257–270

2. Bradford MM (1976) A rapid and sensitive method for the quantitation of microgram quantities of protein utilizing the principle of protein-dye binding. *Anal Biochem* 72(1):248–254
3. Brutus A, Villard C, Durand A, Tahir T, Furniss C, Puigserver A et al (2004) The inhibition specificity of recombinant *Penicillium funiculosum* xylanase B towards wheat proteinaceous inhibitors. *BBA Proteins Proteom* 1701(1):121–128
4. Din N, Damude HG, Gilkes NR, Miller RC, Warren RA, Kilburn DG (1994) C1-Cx revisited: intramolecular synergism in a cellulase. *Proc Natl Acad Sci* 91(24):11383–11387
5. Fujimoto Z, Kuno A, Kaneko S, Kobayashi H, Kusakabe I, Mizuno H (2002) Crystal structures of the sugar complexes of *Streptomyces olivaceoviridis* E-86 xylanase: sugar binding structure of the family 13 carbohydrate binding module. *J Mol Biol* 316(1):65–78
6. Fujimoto Z, Kuno A, Kaneko S, Yoshida S, Kobayashi H, Kusakabe I et al (2000) Crystal structure of *Streptomyces olivaceoviridis* E-86 β -xylanase containing xylan-binding domain. *J Mol Biol* 300(3):575–585
7. Ghangas GS, Hu YJ, Wilson DB (1989) Cloning of a *Thermomonospora fusca* xylanase gene and its expression in *Escherichia coli* and *Streptomyces lividans*. *J Bacteriol* 171(6):2963–2969
8. Jamal-Talabani S, Boraston AB, Turkenburg JP, Tarbouriech N, Ducros VMA, Davies GJ (2004) Ab Initio Structure Determination and Functional Characterization of CBM36: a new family of calcium-dependent carbohydrate binding moles. *Structure* 12:1177–1187
9. Khan MIM, Sajjad M, Sadaf S, Zafar R, Niazi UH, Akhtar MW (2013) The nature of the carbohydrate binding module determines the catalytic efficiency of xylanase Z of *Clostridium thermocellum*. *J Biotechnol* 168:403–408
10. Kittur FS, Mangala SL, Rus'd AA, Kitaoka M, Tsujibo H, Hayashi K (2003) Fusion of family 2b carbohydrate-binding module increases the catalytic activity of a xylanase from *Thermotoga maritima* to soluble xylan. *FEBS Lett* 549(1):147–151
11. Ko CH, Chen WL, Tsai CH, Jane WN, Liu CC, Tu J (2007) *Paenibacillus campinasensis* BL11: a wood material-utilizing bacterial strain isolated from black liquor. *Bioresour Technol* 98(14):2727–2733
12. Kocabaş DS, Güder S, Özben N (2015) Purification strategies and properties of a low-molecular weight xylanase and its application in agricultural waste biomass hydrolysis. *Catal B Enzym* 115:66–75
13. Liu MQ, Dai XJ, Liu GF, Wang Q (2013) Obtaining cellulose binding and hydrolyzing activity of a family 11 hybrid xylanase by fusion with xylan binding domain. *Protein Expr Purif* 88:85–92
14. Liu L, Zeng L, Wang S, Cheng J, Li X, Song A et al (2012) Activity and thermostability increase of xylanase following transplantation with modules sub-divided from hyper-thermophilic CBM9_1-2. *Process Biochem* 47(5):853–857
15. Qiao W, Tang S, Mi S, Jia X, Peng X, Han Y (2014) Biochemical characterization of a novel thermostable GH11 xylanase with CBM6 domain from *Caldicellulosiruptor kronotskyensis*. *Catal B Enzym* 107:8–16
16. Ravalason H, Herpoël-Gimbert I, Record E, Bertaud F, Grisel S, de Weert S et al (2009) Fusion of a family 1 carbohydrate binding module of *Aspergillus niger* to the *Pycnoporus cinnabarinus* laccase for efficient softwood kraft pulp biobleaching. *J Biotechnol* 142(3):220–226
17. Shallom D, Shoham Y (2003) Microbial hemicellulases. *Curr Opin Microbiol* 6:219–228
18. Shin ES, Yang MJ, Jung KH, Kwon EJ, Jung JS, Park SK et al (2002) Influence of the transposition of the thermostabilizing domain of *Clostridium thermocellum* xylanase (XynX) on xylan binding and thermostabilization. *Appl Environ Microbiol* 68:3496–3501
19. Simpson PJ, Bolam DN, Cooper A, Ciruela A, Hazlewood GP, Gilbert HJ, Williamson MP (1999) A family IIB xylan-binding domain has a similar secondary structure to a homologous family IIA cellulose-binding domain but different ligand specificity. *Structure* 7:853–864
20. Sunna A, Gibbs MD, Bergquist PL (2000) A novel thermostable multidomain 1,4-beta-xylanase from *Caldibacillus cellulovorans* and effect of its xylan-binding domain on enzyme activity. *Microbiology* 146:2947–2955
21. Techapun C, Poosaran N, Watanabe M, Sasaki K (2003) Thermostable and alkaline-tolerant microbial cellulase-free xylanases produced from agricultural wastes and the properties required for use in pulp bleaching bioprocesses: a review. *Process Biochem* 38(9):1327–1340
22. Ustinov BB, Gusakov AV, Antonov AI, Sinitsyn AP (2008) Comparison of properties and mode of action of six secreted xylanases from *Chrysosporium lucknowense*. *Enzym Microb Technol* 43:56–65
23. Van Gool MP, Van Muiswinkel GCJ, Hinz SWA, Schols HA, Sinitsyn AP, Gruppen H (2012) Two GH10 endo-xylanases from *Myceliophthora thermophila* C1 with and without cellulose binding module act differently towards soluble and insoluble xyans. *Bioresour Technol* 119:123–132
24. Yan Q, Hao S, Jiang Z, Zhai Q, Chen W (2009) Properties of a xylanase from *Streptomyces matensis* being suitable for xylooligosaccharides production. *Catal B Enzym* 58(1):72–77
25. Zheng H, Liu Y, Han Y, Liu X, Wang J, Han Y, Lu F (2012) Isolation, purification, and characterization of a thermostable xylanase from a novel strain, *Paenibacillus campinasensis* G1-1. *J Microbiol Biotechnol* 22:930–938
26. Zheng H, Liu Y, Liu X, Han Y, Wang J, Lu F (2012) Overexpression of a *Paenibacillus campinasensis* xylanase in *Bacillus megaterium* and its applications to biobleaching of cotton stalk pulp and saccharification of recycled paper sludge. *Bioresour Technol* 125:182–187
27. Zheng HC, Liu YH, Sun MZ, Han Y, Wang JL, Sun JS et al (2014) Improvement of alkali stability and thermostability of *Paenibacillus campinasensis* Family-11 xylanase by directed evolution and site-directed mutagenesis. *J Ind Microbiol Biotechnol* 41:153–162